Post-print of: Ullah U., Kozieł S.: A Broadband Circularly Polarized Wide-Slot Antenna with a Miniaturized Footprint. IEEE ANTENNAS AND WIRELESS PROPAGATION LETTERS. Vol. 17, iss. 12 (2018), pp. 2454 - 2458. DOI: 10.1109/LAWP.2018.2877800

A Broadband Circularly Polarized Wide-Slot Antenna with a Miniaturized Footprint

Ubaid Ullah and Slawomir Koziel, *Senior Member, IEEE*

***Abstract*—This letter presents a novel and simple feeding technique for exciting orthogonal components in a wide-slot antenna. In this technique, a rectangular bracket-shape parasitic strip is placed at the open end of the straight microstrip line to excite the fundamental horizontal and vertical components of the circular polarization (CP). The proposed technique—when employed in conjunction with the asymmetrical geometry of coplanar waveguide (CPW) and a protruded stub from the ground plane—permits for maintaining axial ratio (AR) below 3 dB within a wide range in the C-band as well as a compact footprint of the antenna. All geometry parameters of the antenna are adjusted through rigorous EM-driven optimization to obtain the best performance in terms of footprint, impedance matching, and axial ratio bandwidth (ARBW). The size of the proposed antenna is only 27 mm × 28.8 mm. The structure features a 62 percent impedance bandwidth (3.6 GHz-6.85 GHz) and ARBW of approximately 49 percent (3.6 GHz to 5.93 GHz) with the average realized gain of 3.3 dB within the CP operating band. Numerical results are validated experimentally. Close agreement between simulation and measurement results has been observed.**

***Index Terms*—wide band antennas, compact antennas, wide-slot antennas, EM-driven design, circularly polarized antenna.**

I. Introduction

Development of broadband circularly polarized (CP) antennas with compact geometries and simple topologies have become one of the main research topics for antenna engineers. In modern wireless communication including WLAN, WiMAX, and RFID, CP antennas are preferred due to their excellent features compared to linearly polarized (LP) antennas [1]. Some of these attractive characteristics of CP antennas include reduction of multi-path losses, flexibility in antenna orientation at the transmission and reception end, as well as stable communication links. Recent trends in wireless communication systems are compactness and simultaneous multi-band operation which lead to imposing serious limitations on the physical size but also stringent requirements concerning electrical and field characteristics of the antenna. To comply with these requirements, the antenna has to be compact in size to permit integration into the allocated space within the system, and, at the same time, it should be able to operate in a broadband manner [2], [3].

There have been numerous techniques proposed to launch CP radiation and many CP antenna topologies have been reported in the literature. A commonly used approach for exciting resonant modes with equal amplitudes and orthogonal in phase is by employing a 90-degree power divider, sequentially rotated series feeding networks, or phase delay circuits. These techniques are very effective in achieving a wide axial ratio bandwidth (ARBW), but with the shortcomings of additional circuit complexity and a larger size of the antenna [4]-[6]. Several alternative techniques have been implemented for excitation of CP modes mostly based on an appropriate topological modification of the antenna resonator and the ground plane [7], [8]. In case of planar antennas, various feedline modification has been used to obtain wide ARBW [9], [10]. Among the planar structures, wide-slot antennas have the advantage of low profile, simple geometry, cost-effectiveness, and wider operating bandwidth. Several types of wide-slot antennas with different geometrical configurations have been recently studied in the context of impedance bandwidth and ARBW enhancement [11]-[14]. However, the ARBW reported in these works is only 28.8%, 27%, 41.3%, and 27.45%, respectively. Furthermore, it is achieved at the expense of a relatively larger size and complex excitation mechanism of the CP modes.

In this letter, the aim is to design a simple structure of the feeding network for exciting orthogonal modes while maintaining compact geometry and enhanced ARBW of the antenna. To achieve this goal, we propose a new rectangular bracket-shape parasitic-strip-type feeding technique in combination with an asymmetric coplanar waveguide (CPW) and a wide-slot antenna. By employing the proposed technique as well as rigorous EM-driven optimization of all geometry parameters, a wider ARBW of approximately 49 percent is achieved while maintaining the low-profile structure and a compact size of only 27 mm × 28.8 mm. Comparison with recent state-of-the-art CP designs indicates the superiority of the proposed antenna with respect to ARBW [12-22]. Also, competitive size is achieved despite the topological simplicity of the structure. Numerical results are validated experimentally.

II. Antenna Configuration and Design Analysis

The configuration of the proposed wide-slot antenna is illustrated in Fig 1. The antenna is designed on an Arlon AD250C substrate (ε_r = 2.5, tanδ = 0.0014, h = 0.762 mm). For antenna excitation, a coplanar waveguide (CPW) with 50Ω straight

Manuscript submitted on March 21, 2018. This work was supported in part by the Icelandic Centre for Research (RANNIS) Grant 174114051, by the National Science Centre of Poland Grant 2014/15/B/ST7/04683.

U. Ullah and S. Koziel are with Engineering Optimization and Modeling Center of Reykjavik University, Reykjavik, Iceland (e-mail: ubaidu@ru.is); S. Koziel is also with the Faculty of Electronics, Telecommunications and Informatics, Gdansk University of Technology, 80-233 Gdansk, Poland (e-mail: koziel@ru.is).

This article has been accepted for publication in a future issue of this journal, but has not been fully edited. Content may change prior to final publication. Citation information: DOI 10.1109/LAWP.2018.2877800, IEEE Antennas and Wireless Propagation Letters

microstrip feed line with a length L_m and a rectangular bracket-shape parasitic strip is employed. An asymmetrical configuration of the coplanar ground planes in both *x-axis* and *y*-axis is used, and a horizontal strip is added to the ground plane below the feedline. The width of the parasitic strips and the horizontal strip in the ground plane is kept to 1 mm. The computational model of the antenna is implemented in CST Microwave Studio.

A. *Antenna Development Stages*

The antenna development stages are shown in Fig. 2. In the first step, a straight-line monopole antenna with the length of an approximately quarter wavelength is designed to generate the fundamental resonance at near the center frequency as shown in Fig. 2. At this stage, there are no CP components and the antenna is perfectly linearly polarized as shown. In the second design stage, an inverted rectangular bracket-shape parasitic strip is loaded at the open end of the microstrip line with the horizontal distance d_1 and the vertical distance d_2 so as to have sufficient coupling to the source line for exciting the fundamental CP mode at the upper frequency band as shown in Fig. 3(b).

In the third design stage, a horizontal strip is added to the ground plane in the *x*-direction and the symmetry of the co-planar ground plane is adjusted in +*y*-direction to enhance the impedance matching and to generate an additional CP mode at the lower frequency as illustrated. In the final design stage, the symmetry of the ground along the *x*-direction and, at the same time, the parameters L_2 and L_4 are attuned to merge all the resonances and CP modes at the lower and upper bands.

The impedance matching and ARBW for the fourth stage as depicted in Fig. 2 are achieved after optimization of all geometry parameters of the antenna. The optimization process has been oriented towards improving the axial ratio of the antenna with the constraint on its reflection response (to keep it under –10 dB within the intended operational bandwidth). The optimization algorithm utilized was a trust-region gradient search [23] with numerical derivatives and the constraint handling was implicit (by means of penalty functions [24]). This type of constraint handling works better than explicit handling due to the constraint being computationally expensive. More specifically, the constraint is typically active at the optimum design, which, in conjunction with the numerical noise inherent to EM simulation results makes explicit treatment inefficient.

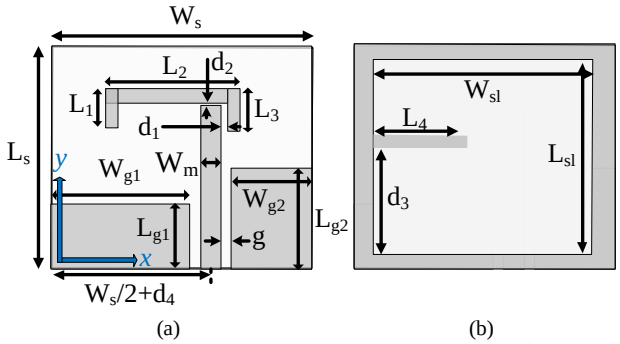

Fig. 1. Configuration of the proposed antenna: (a) parameterized front view (b) parameterized back view. The substrate and metallization are marked using the light and dark-shade gray, respectively.

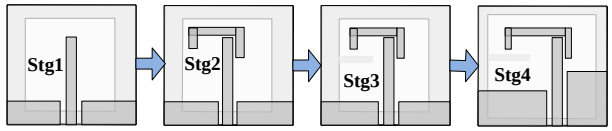

Fig. 2. Development stages of the proposed CP antenna.

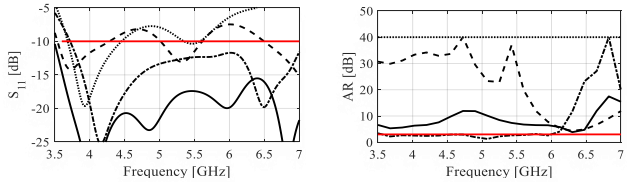

Fig. 3. Antenna characteristics through the evolution stages: Stage 1 (….), Stage 2 (----), Stage 3(——), and Stage 4 (- · - · -): (a) $|S_{11}|$, (b) AR.

B. *Antenna Analysis through Parameters*

Fig. 4 illustrates the effects of the ground plane symmetry on impedance matching S_{11} and axial ratio AR. The effects of the parameter L_{g1} on AR and S_{11} are shown in Fig. 4(a-b) by varying it from 5 mm (initial value) to 9 mm with 1 mm step along the *y*-direction in the range. It can be observed that L_{g1} mostly effects the upper-frequency band. Some variations can also be seen in the lower band; however, AR stays within the acceptable limit below 3dB. The variation of the parameter L_{g2} along the *y*-direction (cf. Fig. 4(c-d)) indicates that the central CP band is lowered from more than 10 dB to below 3 dB with the increase in length from 11 mm to 15 mm. Fig. 4(e-f) indicates the effect of the asymmetry in the *x*-direction controlled by the parameter d_4 (here, varying from 2mm to 6 mm with a 1 mm step) on AR and S_{11}. The parameter L_2 (length of the horizontal parasitic strip) is directly dependent on d_4, so when d_4 increases, L_2 increases as well. The initial value of L_2 was fixed at 10 mm and simultaneously varied with d_4 up to 15mm. The results clearly show that the upper CP mode is reliant on the values of d_4 and L_2 and can be attuned to below 3 dB by proper parameter adjustment. Finally, Fig. 4(g-h) illustrates the effects of varying the length L_4 (length of the horizontal strip in the ground plane) on AR and S_{11} in the lower frequency of the CP operating mode. The variation of the length from 5 mm to 10 mm with a 1 mm step depicts that by increasing L_4 a drastic enhancement in the lower CP band can be achieved within this range. The effect of varying the horizontal d_1 and vertical d_2 spacing can be seen in Fig. 4 (i-l). As these parameters primarily control the coupling from the microstrip line to the parasitic bracket shape strip, a sensitivity analysis is performed by varying these dimensions from 0 mm to 1 mm. A slight variation in the AR performance is observed particularly in the upper frequency band. The impedance matching is marginally effected but remains within the acceptable –10 dB level.

From the above analysis, it is concluded that the aforementioned parameters play a vital role in attaining a broad impedance bandwidth as well as ARBW. In order to ensure the best possible antenna performance, all geometry parameters of the antenna have been tuned through rigorous numerical optimization at the full-wave EM level of description. The final optimized parameter values are listed in Table I.

This article has been accepted for publication in a future issue of this journal, but has not been fully edited. Content may change prior to final publication. Citation information: DOI 10.1109/LAWP.2018.2877800, IEEE Antennas and Wireless Propagation Letters

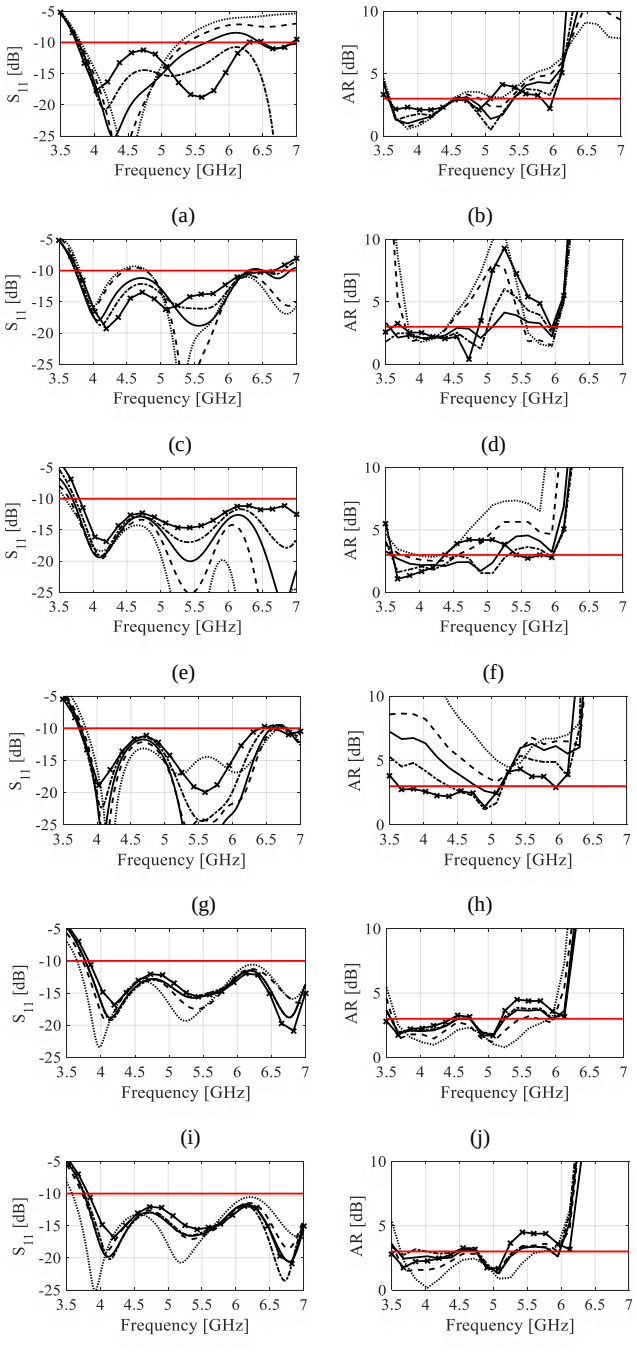

Fig. 4. Parameter effects on impedance matching and axial ratio: Step 1 (….), Step 2 (----), Step 3 (——), Step 4 (- · - ·), and Step 5 (-x-x-x): (a) L_{g1} (|S_{11}|), (b) L_{g1} (AR), (c) L_{g2} (|S_{11}|), (d) L_{g2} (AR), (e) d_4 (|S_{11}|), (f) d_4 (AR), (g) L_4 (|S_{11}|), (h) L_4 (AR), (i) d_1 (|S_{11}|), (j) d_1 (AR), (k) d_2 (|S_{11}|), (l) d_2 (AR)

TABLE I OPTIMIZED PARAMETER VALUES

Parameter	Value	Parameter	Value	Parameter	Value
L_s	27.00	L_{sl}	25.00	L_3	3.13
W_s	28.80	W_{sl}	24.30	L_4	9.98
L_{g1}	8.64	L_m	19.00	d_1	0.68
W_{g1}	18.04	W_m	1.80	d_2	0.34
L_{g2}	13.23	L_1	2.71	d_3	14.15
W_{g2}	7.95	L_2	14.98	d_4	5.04
g	0.50				

C. *Surface Current Distribution of Circular Polarization*

To analyze the CP mechanism of the antenna, the time varying simulated surface currents in Fig. 5 are exmined at 5 GHz which is close to the center frequency (f_c) of the ARBW. At 0 degrees, the current is predominantly directed in the +*x*-direction, whereas at 90 degrees, the direction of the dominant components of the current changes to the +*y*-direction. Moreover, at 180 degrees, the direction of the current again changes to –*x*-direction and for 270 degrees the direction of the current changes to -*y*-direction. The intensities of the current are shown with the same scales from which it can be inferred that the amplitudes for all four instances are almost the same. It should also be mentioned that while the dominant currents occur in the desired directions as indicated in Fig. 5, a noticeable current component in the *x*-direction can also be observed for 90 and 270 degrees (Fig. 5(b),(d)), which contributes to a slight AR degradation. This current may be attributed to the low dielectric constant value of the substrate used for antenna implementation. As the surface current located at the azimuth is rotating in an anticlockwise direction when observed from +*z*-direction, therefore right-hand circular polarization (RHCP) is obtained at 5.0 GHz.

III. EXPERIMENTAL VALIDATION

The final optimized design has been fabricated and validated experimentally in an anechoic chamber. A photograph of the antenna prototype is shown in Fig. 6. An excellent agreement between simulation and measured results can be observed. The simulated and measured impedance bandwidths is as wide as 62 percent (3.6 GHz to 6.85 GHz) as illustrated in Fig. 7(a). The axial ratio response is plotted in Fig. 6(b), whereas ARBW of 49 percent (3.6 GHz to 5.93 GHz) is achieved in the broadside direction (i.e., for $\theta = 0$ and $\varphi = 0$). The simulated and measured realized gains in the ±*z*-direction of the antenna is demonstrated in Fig. 8. A relatively stable response in the CP operating band with an average gain of 3.3 dB is achieved.

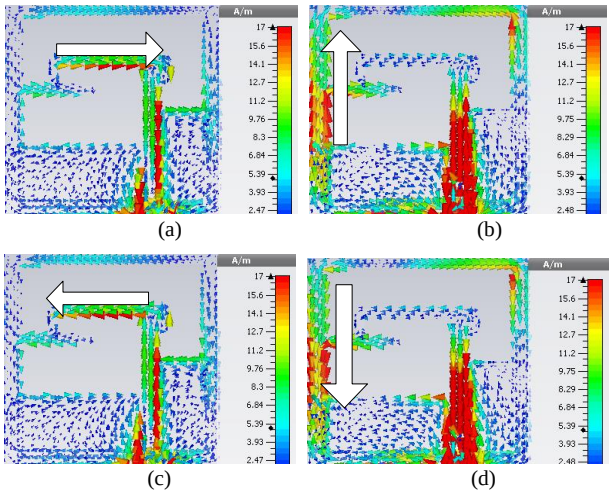

Fig. 5. Surface current distributions at 5.0 GHz: (a) 0 degrees, (b) 90 degrees, (c) 180 degrees, (d) 270 degrees.

This article has been accepted for publication in a future issue of this journal, but has not been fully edited. Content may change prior to final publication. Citation information: DOI 10.1109/LAWP.2018.2877800, IEEE Antennas and Wireless Propagation Letters

The radiation patterns characteristics of the proposed antenna at different frequencies in *xz*-plane are shown in Fig 9. CP with the opposite sense is realized in +*z*-direction and –*z*-direction with close agreement between simulation and measurement. Fig. 10 shows the simulated and measured efficiencies of the antenna with a good agreement between the two data sets. It can be observed that the average efficiency within the entire operating range of the antenna is approximately 95%.

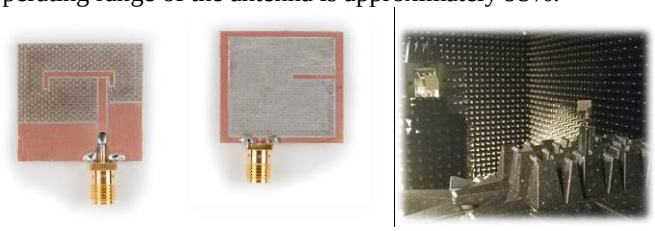

(a) (b) (c)

Fig. 6. Photograph of the fabricated antenna prototype: (a) top view, (b) bottom view, (c) experimental setup.

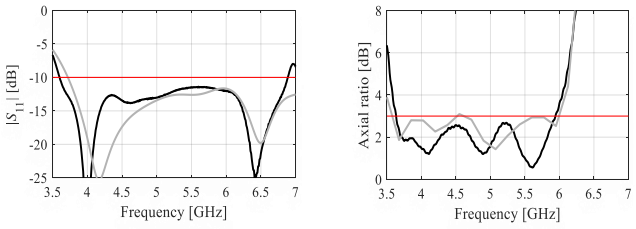

(a) (b)

Fig. 7. Simulated (gray) and measured (black) characteristics of the proposed antenna: (a) $|S_{11}|$, (b) AR.

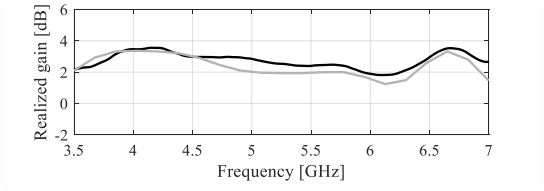

Fig. 8. Simulated (gray) and measured (black) realized gains in the broadside direction.

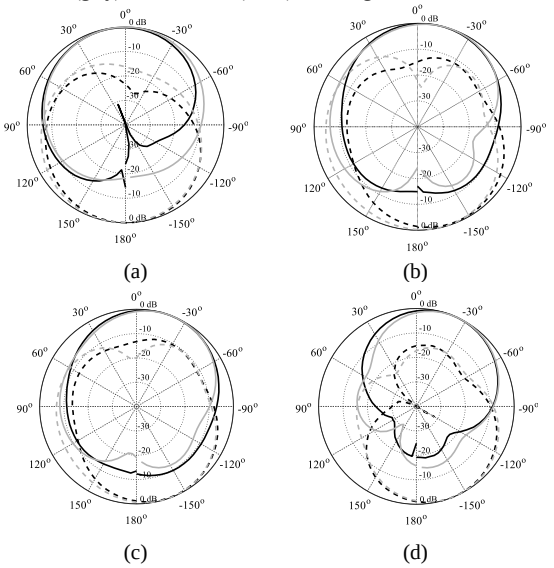

(a) (b) (c) (d)

Fig. 9. Simulated (gray) and measured (black) radiation patterns of the proposed CP antenna with RHCP (solid) and LHCP (dashed). (a) 3.8 GHz, (b) 5 GHz, (c) 5.2 GHz, and (d) 5.8 GHz.

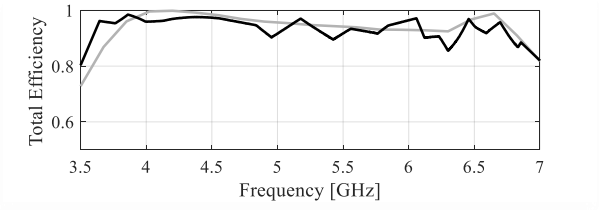

Fig. 10. Simulated and measured efficiencies of the proposed antenna, simulated (gray), and measured (black).

TABLE II COMPARISON WITH STATE-OF-THE-ART CP ANTENNAS

Ref	%AR	%BW	Size [λ_o^2]	Substrate (h (mm), ε)
[7]	30	51	1.38	….(2.2, 1.6)
[12]	27	50.2	0.23	FR4 (1.6,4.4)
[13]	41.3	84	0.28	RT(1.6, 2.2)
[14]	27.45	71.63	0.42	FR4 (1.6,4.4)
[15]	39.4	57	0.78	AD(0.762, 2.5)
[16]	40	90.2	0.28	FR4 (1.6,4.4)
[17]	27	111	0.38	FR4 (0.8, 4.4)
[18]	15.4	----	0.31	FR4 (1,4.4)
[19]	26.9	27	1.02	FR4(1.6,4.4)
[20]	14	27	0.13	FR4 (0.8, 4.4)
[21]	22	37	0.89	RT(0.8, 4.4)
[22]	42	55.5	0.15	FR4 (1,4.4)
Proposed	~49	62	0.20	AD(0.762, 2.5)

For benchmarking, the proposed antenna has been compared with recent state-of-the-art CP designs. The data gathered in Table II indicates that our design exhibits better performance in terms of ARBW, and, in most cases, much smaller size than the reference antennas. The size comparisons are performed based on f_c of the AR at the free space wavelength (λ_o).

IV. CONCLUSION

A novel technique for exciting orthogonal modes, applied to realize a broadband circular polarization antenna with compact geometry, has been presented. A simple rectangular bracket-shape parasitic strip is used to excite the CP modes and to further enhance them by using the asymmetrical geometry of CPW coplanar ground planes and an additional straight strip in the wide-slot. With the proposed technique, both a compact geometry and wide ARBW can be achieved. All geometrical parameters were adjusted by means of a rigorous numerical optimization. As a result, a wide impedance bandwidth of 61 percent and ARBW of 49 percent is achieved while maintaining a compact size of the antenna. The final design has been validated experimentally with a close agreement between simulations and measurements demonstrated. Comprehensive benchmarking demonstrates that the considered antenna outperforms recently reported designs with respect to ARBW as well as the impedance bandwidth among the structures featuring similar size. The application area of the proposed antenna includes several WLAN and WiMAX bands.

ACKNOWLEDGMENT

The authors would like to thank Dassault Systemes, France, for making CST Microwave Studio available.

This article has been accepted for publication in a future issue of this journal, but has not been fully edited. Content may change prior to final publication. Citation information: DOI 10.1109/LAWP.2018.2877800, IEEE Antennas and Wireless Propagation Letters

REFERENCES

[1] R. Xu, J. Li, and J. Liu, "A Design of Broadband Circularly Polarized C-Shaped Slot Antenna with Sword-Shaped Radiator and Its Array for L/S-Band Applications", *IEEE Access*, Vol. 6, pp. 5891-5896, 2018.

[2] R. Zaker and A. Abdipour, "A very compact ultrawideband printed omnidirectional monopole antenna," *IEEE Antennas Wireless Propag. Lett*., vol. 9, pp. 471–473, 2010.

[3] E. Arnieri, L. Boccia, G. Amendola, and G. D. Massa, "A compact high gain antenna for small satellite applications," *IEEE Trans. Antennas Propag*., vol. 55, no. 2, pp. 277–282, Feb. 2007.

[4] M. Shokri, V. Rafii, S. Karamzadeh, Z. Amiri, and B. Virdee, "Miniaturised ultra-wideband circularly polarised antenna with modified ground plane," Electron. Lett., vol. 50, no. 24, pp. 1786–1788, 2014.

[5] U. Ullah, M. F. Ain, and Z. A. Ahmad, "A review of wideband circularly polarized dielectric resonator antennas," *China Commun.,* vol. 14, no. 6, pp. 65-79, 2017.

[6] Y.-M. Cai, K. Li, Y.-Z. Yin, and W. Hu, "broadband circularly polarized printed antenna with branched microstrip feed," IEEE Antennas Wireless Propag. Lett., vol. 13, pp. 674–677, 2014.

[7] T. Kumar and A. R. Harish, "Broadband Circularly Polarized Printed Slot-Monopole Antenna," *IEEE Antennas Wireless Propag. Lett*., vol. 12, pp. 1531-1534, 2013.

[8] R. C. Han, and S.-S. Zhong, "Broadband circularly-polarised chifreshaped monopole antenna with asymmetric feed," Electron. Lett., vol. 52, no. 4, pp. 256–258, Feb. 2016.

[9] G. Feng, L. Chen, X. Xue and X. Shi, "Broadband Circularly Polarized Crossed-Dipole Antenna with a Single Asymmetrical Cross-Loop," *IEEE Antennas Wireless Propag. Lett*., vol. 16, pp. 3184-3187, 2017

[10] K. Ding, C. Gao, T. Yu and D. Qu, "Broadband C-Shaped Circularly Polarized Monopole Antenna," *IEEE Trans. Antennas Propag.,* vol. 63, no. 2, pp. 785-790, Feb. 2015.

[11] J. Y. Sze and C. C. Chang, "Circularly polarized square slot antenna with a pair of inverted-L grounded strips," *IEEE Antennas Wirel. Propag. Lett.,* vol. 7, pp. 149–151, 2008.

[12] Y. He, W. He and H. Wong, "A Wideband Circularly Polarized Cross-Dipole Antenna," *IEEE Ant. Wireless Propag. Lett*., vol. 13, pp. 67-70, 2014.

[13] M. Nosrati and N. Tavassolian, "Miniaturized Circularly Polarized Square Slot Antenna With Enhanced Axial-Ratio Bandwidth Using an Antipodal Y-strip," *IEEE Antennas Wireless Propag. Lett*.,, vol. 16, pp. 817-820, 2017.

[14] R. K. Saini, S. Dwari, and M. K. Mandal, "CPW-Fed Dual-Band Dual-Sense Circularly Polarized Monopole Antenna," *IEEE Antennas Wireless Propag. Lett*., vol. 16, pp. 2497-2500, 2017.

[15] H. G. Xue, X. X. Yang and Z. Ma, "A Novel Microstrip-CPW Fed Planar Slot Antenna With Broadband and Circular Polarization," *IEEE Antennas Wireless Propag. Lett*., vol. 14, pp. 1392-1395, 2015.

[16] M. S. Ellis, Z. Zhao, J. Wu, X. Ding, Z. Nie and Q. H. Liu, "A Novel Simple and Compact Microstrip-Fed Circularly Polarized Wide Slot Antenna With Wide Axial Ratio Bandwidth for C-Band Applications," *IEEE Trans. Antennas Propag.*, vol. 64, no. 4, pp. 1552-1555, April 2016.

[17] J.Y. Jan, C.Y. Pan, K.Y. Chiu, and H.M Chen, "Broadband CPW-fed circularly-polarized slot antenna with an open slot," *IEEE Trans. Antennas Propag.*, vol. 61, no. 3, pp. 1418-1422, 2013.

[18] G. Beigmohammadi, C. Ghobadi, J. Nourinia, and M. Ojaroudi, "Small square slot antenna with circular polarisation characteristics for WLAN/WiMAX applications," *Electron. Lett.*, vol. 46, no. 10, pp. 672-673, 2010.

[19] R. Chowdhury, R. Kumar, and R. K. Chaudhary, "A coaxial probe fed wideband circularly polarized antenna using unequal and adjacent-slided rectangular dielectric resonators for WLAN applications," *Int J. RF Microw. Comput. Aided Eng*., pp. 1–9, 2017.

[20] Y. Ojaroudi, N. Ojaroudi, N. Ghadimi, "Circularly polarized microstrip slot antenna with a pair of spur-shaped slits for WLAN applications," *Microw. Opt. Technol. Lett*., vol. 57, pp. 756–759, 2015.

[21] S. Fakhte, H. Oraizi, R. Karimian, R. Fakhte, "A new wideband circularly polarized stair-shaped dielectric resonator antenna," *IEEE Trans. Antennas Propag.*,vol. 63, no. 4, pp. 1828-1832, 2015.

[22] K. O. Gyasi, G. Wen, D. Inserra, Y. Huang, J. Li, A. E. Ampoma , and H. Zhang, "A Compact Broadband Cross-Shaped Circularly Polarized Planar Monopole Antenna With a Ground Plane Extension", *IEEE Antennas Wireless Propag. Lett*., vol. 17, no. 2, pp. 335-338, 2018.

[23] A.R. Conn, N.I.M. Gould, and P.L. Toint, *Trust Region Methods*, MPS-SIAM Series on Optimization, 2000.

[24] A. Bekasiewicz, and S. Koziel, "Structure and computationally-efficient simulation-driven design of compact UWB monopole antenna," *IEEE Antennas and Wireless Prop. Lett.*, vol. 14, pp. 1282-1285, 2015.